Bull Volcanol (1990) 52:460-474

Bulletin of
Volcanology

Maximum entropy spectral analysis of volcanic tremor using data from Etna (Sicily) and Merapi (central Java)

D Seidl [1], SB Kirbani [2], and W Brüstle [3]

[1] Central Seismological Observatory Gräfenberg, Krankenhausstrasse 1, D-8520 Erlangen, Federal Republic of Germany
[2] Physics Department, Gadjah Mada University, Yogyakarta, Indonesia
[3] Institute for Geophysics, Richard-Wagner-Strasse 44, D-7000 Stuttgart, Federal Republic of Germany

Received June 2, 1989/Accepted April 4, 1990

Abstract. The maximum entropy spectral analysis (MESA) method is applied to synthetic and observed tremor time series using autoregressive processes and recordings from the volcanoes Etna (Sicily) and Merapi (central Java). The MESA analysis can be used to estimate power spectra with sharp peaks from short data records. If the tremor source process can be modelled by an autoregressive process, the MESA method is well-suited for determining the coefficients of the underlying difference equations. As in the standard periodogram method of power spectrum estimation, a mesagram estimate using record segmentation and MESA spectrum averaging reduces the variance of the spectral estimator. In combination with periodogram estimates, mesagram estimates confirm that the tremor source may be modelled as an ensemble of randomly excited resonators. Used together, these estimates provide a valuable method for short-term monitoring of volcanic activity. In addition, they can be applied to the determination of new source parameters such as resonator frequencies, damping coefficients, excitation probabilities, correlation of exciting forces, and resonator coupling and in the pattern recognition of source types.

Introduction

Near many active volcanoes a persistent seismic wave field of volcanic tremor can be observed. Figure 1 illustrates some characteristics of tremor in the time and frequency domain using observations from Etna (Sicily). Tremor recordings can be regarded as random time series. The long-term power spectrum (analysis interval of tens of minutes to several hours) usually shows many sharp peaks in the frequency range below 10 Hz. The frequencies of the dominant peaks may remain nearly constant for a long time indicating a steady-state tremor source. During periods of increasing eruptive activity a frequency shift of several peaks is usually observed. Transients (wave groups) superimposed on stationary tremor and nonstationary intervals such as tremor storms (Fig. 11 and Fig. 12) show a similar pattern for many volvanoes and can often be correlated with changes in the visible volcanic activity.

The random ground motion of tremor can be caused either by wave scattering or a random source. In the highly inhomogeneous structure of a volcano, scattering is expected to be an important process for tremor wave propagation. The dominant peak frequencies in the power spectrum, however, show only a small dependence on azimuth and distance from the crater (e.g., Riuscetti et al. 1977). This suggests that the peaked spectrum is mainly a source and not a path effect. The dominant effects of scattered waves on the spectrum are probably confined to the frequency range above 10 Hz.

Random ground motion can arise from a random source in two ways: Superimposed wave groups are radiated either by an ensemble of many unrelated sources (like short period seismic noise) or by a random source (like oceanic microseisms produced by fluctuating atmospheric pressure on the ocean). A variety of tremor source models of both types have been suggested for various depth ranges and states of activity. An overview was given by Schick (1988). The basis features of the many models which consider fluctuating magma flow as the primary source of volcanic tremor can be grouped in the resonator model: A weakly damped (high-Q) resonator (the magma-filled conduit) is excited to acoustic resonances by a random series of pulses (random perturbations of the magma conduit pressure field). The response (tremor) is represented as a random sequence of the superimposed impulse response functions of the resonator. If the spectrum of the random input is flat within the bandwidth of the resonator (white noise excitation) than the power spectrum of the tremor corresponds to the squared amplitude response of the resonator. The peak frequency and the bandwidth are determined by the physical parameters of the resonator (geometry and size of the conduit, density and viscosity of the magma, etc.). The peak am-

Offprint requests to: D Seidl

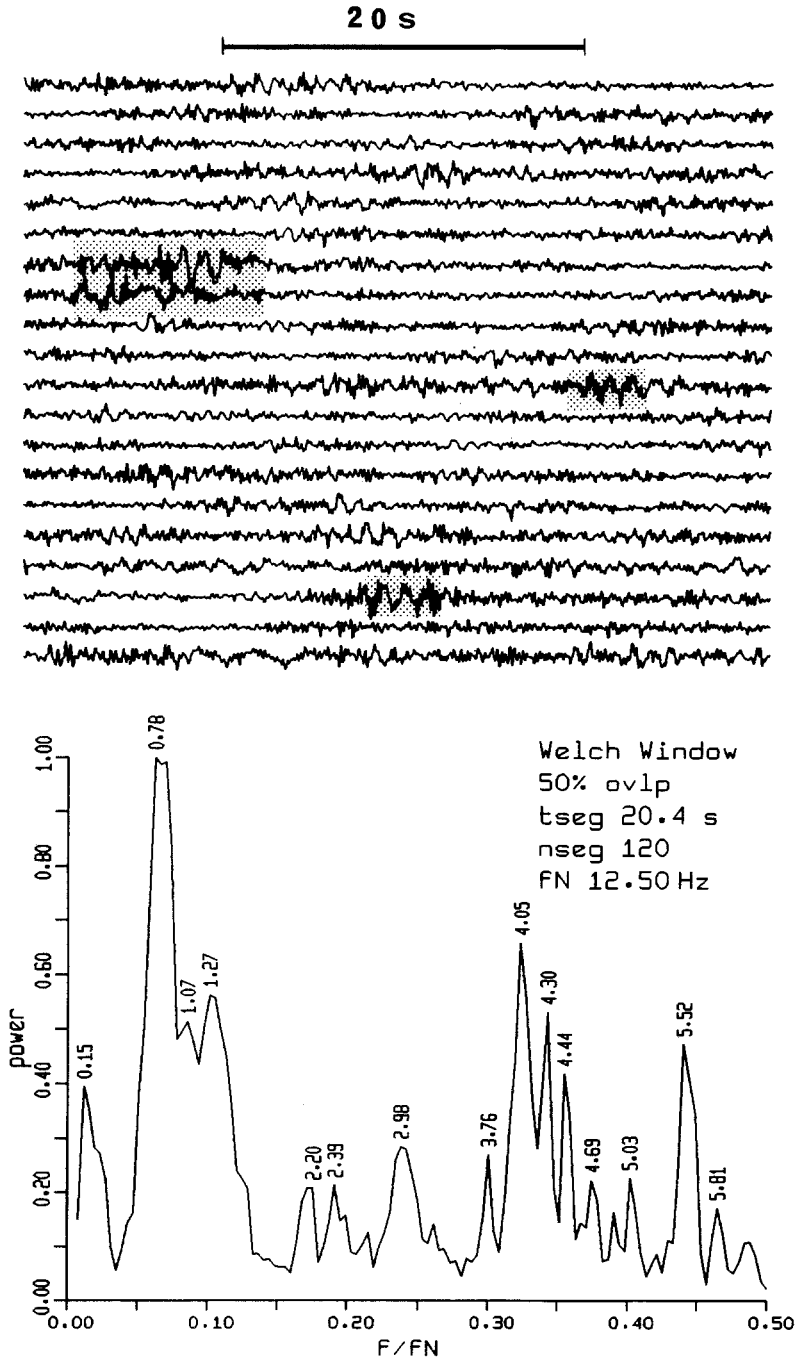

Fig. 1. Two basic properties of volcanic tremor in time and frequency domain: quasi-stationary *random* time series with superimposed transients (wave groups, pointed) and *multipeak* power spectrum. *Top.* Section (length 13.7 min) of tremor recording made at Torre del Filosofo, Etna (Sicily) 1.4 km from crater on 11 July 1988. State of activity, normal; broadband displacement between 0.05 Hz and 5 Hz (Wielandt-Streckeisen seismometer). *Bottom.* Normalized power spectrum. Periodogram estimate using record segmentation, Welch windowing, and segment overlapping by one-half of segment length. The numbers indicate the peak frequencies in Hz. tseg, segment length; nseg, number of data sgements; (number of analyzed overlapped segments 2 nseg-1); f_N, Nyquist frequency

plitude is related to the total power (variance) of the driving random process.

The observed multipeak spectrum results from an ensemble of resonators excited by independent or partially correlated driving forces (resonator-ensemble model). The power spectrum $P(f)$ then has the meaning of a spectral distribution function of the total radiation power. $P(f)\,df$ can be interpreted as the product "excitation probability" (average number of pulses per time unit) times "mean radiation power" of the resonators in the frequency interval $\{f, f+df\}$.

With the advent of digital broadband seismographs, methods developed for other areas of time series analysis may be applied to the two areas of volcanic tremor investigations, i.e., activity monitoring and source parameter determination. Maximum entropy spectral analysis (MESA) is an effective method for the estimation of peaked power spectra from short time intervals. For monitoring nonstationary tremor such as transitions from noneruptive to eruptive activity or stationary tremor superimposed by signal-shaped events, MESA is superior to standard long-term methods of power spectral analysis. Assuming it is reasonable to model a tremor source as an autoregressive process, MESA estimates the coefficients of the underlying difference equations. The determination of the corresponding source parameters may be considered the inversion problem of MESA tremor analysis.

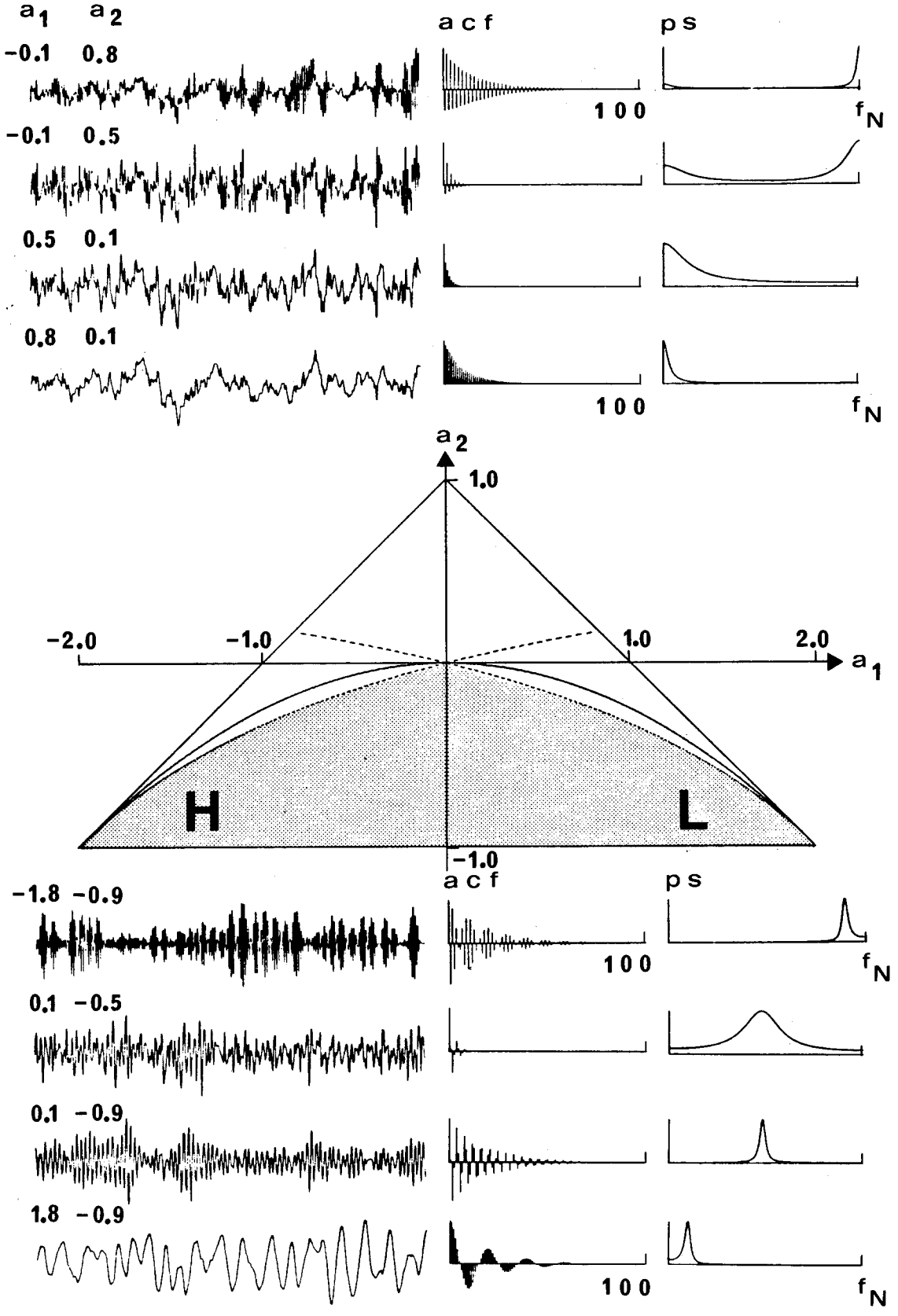

Fig. 2. Modelling of synthetic tremor with second-order autoregressive $AR(2)$ processing using random numbers as input time series. The AR parameters (a1, a2) which generate peaked high-frequency (H) and low-frequency (L) power spectra (*ps*) and damped sine-wave autocorrelation functions (*acf*) are located in the dotted part of the triangle-shaped stability region for $AR(2)$ processes. Length of time series, 500 samples; length of *acf*, 100 lags; frequency interval for *ps*, zero to f_N (Nyquist frequency)

Maximum entropy spectral analysis of synthetic tremor

All resonator-type models describe the tremor as the output of a randomly excited source for seismic waves. The power spectrum $P(f)$ of the recorded tremor is given in frequency (f) domain by

$$P(f)=|H(f)|^2 P_0(f), \tag{1}$$

where $P_0(f)$ is the source power spectrum of the tremor and $H(f)$ is the transfer function of the propagation path. A wide class of linear, random processes x_t (tremor) can be represented in discrete form by the difference equation of an autoregressive process of order p ($AR(p)$ process):

$$x_t=a_1 x_{t-1}+a_2 x_{t-2}+\ldots+a_p x_{t-p}+r_t, \tag{2}$$

where the parameters a_k are constants of the system (magma-filled conduits) and r_t is a purely random (white noise) process (fluctuating magma flow).

The power spectrum of the $AR(p)$ process in Eq. (2) is

$$P(f)=\frac{2s_r^2\,dt}{|1-\sum_{k=1}^{p} a_k \exp(-2\pi i k f dt)|^2}, \tag{3}$$

where s_r is the total power of the input sequence r_t and dt is the sampling interval. The spectrum is continuous in the frequency interval $0\leq f\leq f_N$ with the Nyquist frequency $f_N=1/(2\,dt)$. References on theory, analysis, and simulation of autoregressive discrete time series are, for example, Jenkins and Watts (1969), Box and Jenkins (1976), and Priestly (1981).

Figure 2 shows that a large variety of time series, autocorrelation functions, and power spectra can be simulated using a second-order AR process and a random number generator for the input sequence r_t in Eq. (2). The $AR(2)$ process describes the movement of a randomly excited second-order oscillator, e.g., a pendulum with damping proportional to the velocity. Given the frequency and bandwidth of a spectral peak, an $AR(2)$ process can be fitted to the spectrum by determining the parameters a1 and a2 in the subregion for peaked spectra within the stability triangle in Fig. 2. From a1 and a2 the resonator parameters eigenfrequency and damping coefficient can be calculated. The problem of fitting an ensemble of second-order resonators to a multipeak power spectrum such as in Fig. 1 can therefore be solved by overlapping a finite number of $AR(2)$ processes.

The maximum entropy spectral analysis provides a method for the estimation of power spectra for time series which can be represented by autoregressive (AR) processes. The method was suggested by Burg (1967) and was formulated by Andersen (1974) as a very efficient recursive algorithm. Two volumes with collected contributions on the MESA method have been edited by Childers (1978) and Haykin (1979). Concise treatments including Fortran subroutines are given by Clearbout (1976), Kanasewich (1981), and Press at al. (1986). The application to synthetic and geophysical time series was investigated, for example, by Chen and Stegen (1974), Gutowski et al. (1975), and Ulrych and Bishop (1975).

The method of Burg (1967) determines the parameters of an AR-process of order p directly form the data and calculates the power spectrum by applying Eq. (3). The MESA method has been found to be very efficient in resolving power spectra with sharp peaks from short data records. The main shortcomings at present are the lack of practical methods for determining a suitable order p and a variance estimate. The application of MESA to tremor data shows that these problems can be partially solved by interpreting the MESA short-term spectra together with the long-term periodogram spectrum.

Figure 3 demonstrates the application of MESA to a synthetic $AR(2)$ process generated with normally distributed random numbers as the input time series. First, the order of an optimal autoregressive representation for the time series must be determined. Although different criteria have been proposed by various authors (e.g., Haykin 1979), the final prediction-error criterion suggested by Akaike (1974) is used here. It is based on the equivalence between an $AR(p)$ process and a prediction filter of order p. According to this criterion the order m which gives the minimum of an estimator called the final prediction error (FPE) in terms of m is used as optimal value. In Fig. 3 log[FPE(m)] has a break in the curve for the correct order $m=2$ and a nearly constant value for higher orders. The second-order MESA spectra for subsequent segments of the time series exhibit only small variations in shape, but large fluctuations in total power around the true spectrum caused by the high sensitivity of the total power to small changes of the parameters. The variance of the spectral estimate can be reduced by averaging the segment spectra. The spectral estimate obtained by sectioning the time series and averaging the segment MESA spectra is called a mesagram. The examples in Fig. 3 indicate that for a given order, the mesagram tends to the true spectrum and the averaged AR parameter tend to the true values if the number of segments is increased.

Figure 4 illustrates the application of MESA to a synthetic autoregressive process of two superimposed $AR(2)$ processes with peaked spectra. If the process has two separated peaks, the FPE criterion gives the order $m=4$ and the corresponding two-segment mesagram provides a good estimation of the true spectrum. For the double-peak case the break point value in the FPE(m) curve can no longer resolve the peaks. A higher order must be used to resolve the double peak. In general, three intervals can be observed along the m-axis: a low-order interval with increasing resolution for increasing order, an intermediate interval with stable spectra, and a high-order interval with unstable spectra showing splitting effects with spurious peaks, mainly due to round-off errors. The stability of the spectrum in terms of the order m and the comparison of the mesagram spectrum with the long-term periodogram power

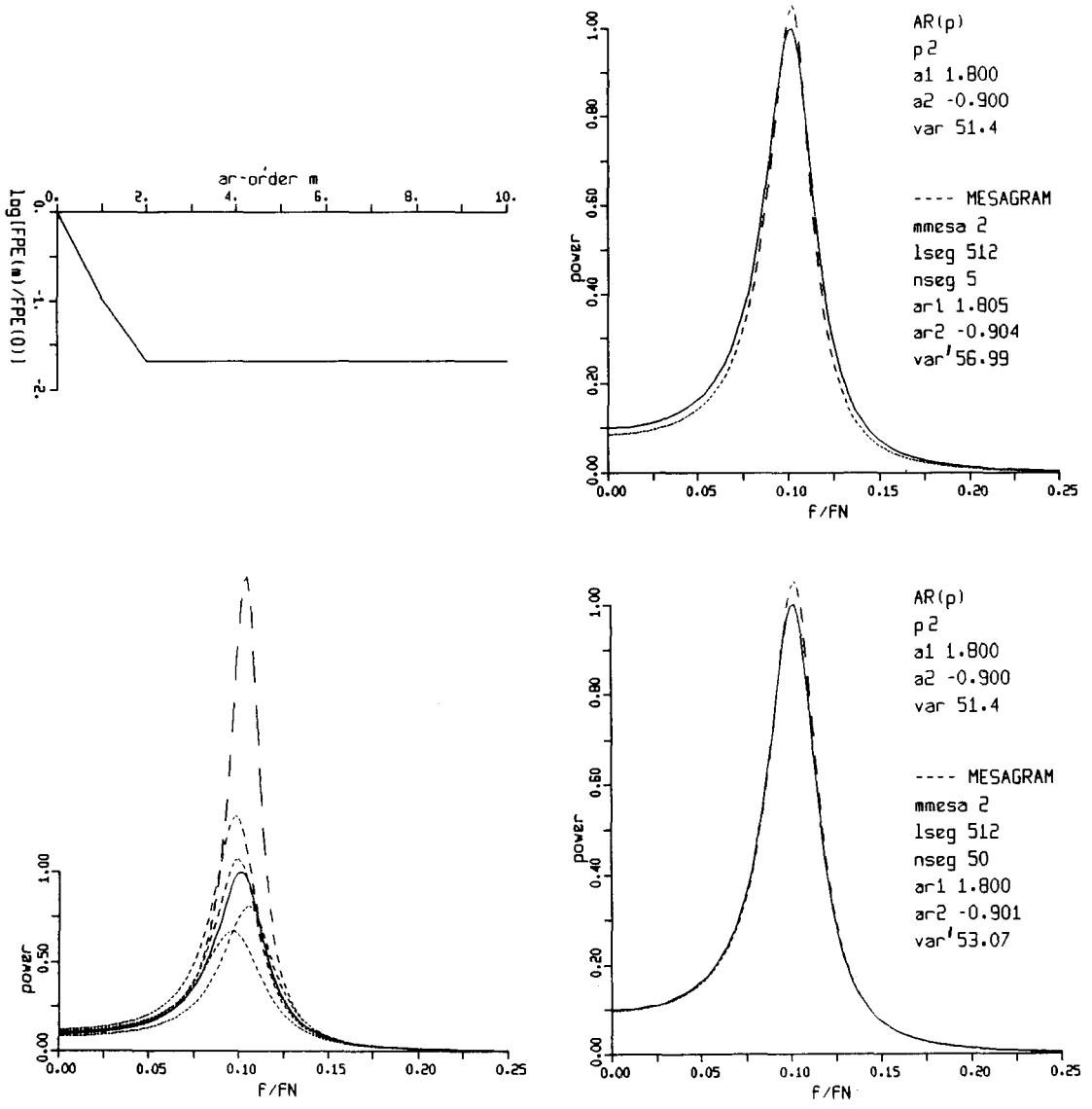

Fig. 3. Maximum entropy spectral analysis of a synthetic $AR(2)$ process with peaked power spectrum using the mesagram estimate. *Left top.* Determination of the order of the AR process using the final prediction error (*FPE*) criterion. *Left bottom.* Fluctuations of single segment MESA spectra (order mmesa = 2; dashed) around the theoretical spectrum (solid). *Right.* Variance reduction by record segmentation and averaging the segment MESA spectra (mesagram estimate). a1, a2, parameters of $AR(2)$ process; var, total power of $AR(2)$ process; lseg, segment length in samples; p, order of synthetic AR process; m, order of MESA estimator; mmesa, particular order of m for MESA spectra; nseg, number of segments for mesagram estimation; ar1, ar2, estimated $AR(2)$ parameters (averaged from nseg segments); var', estimated total power (averaged from nseg segments)

spectrum are two empirical criteria for a significance check of spectral peaks.

Figure 5 compares the mesagram with the standard periodogram approach. The mesagram provides a smoother and more stable estimate of the true spectrum by averaging a smaller number of segments.

Spectral analysis of volcanic tremor recordings

Assuming a resonator-ensemble model, the tremor time series will depend mainly on two factors. One of these is the number of resonators, N. The other factor is the relationship between the decay times t_c of the resonator impulse response functions and the average time intervals t_e between two successive excitations. For $N=1$ and $t_e < t_c$, the overlapping response functions generate a continuous wave train. The time series of a second-order resonator can then take on any of the forms shown in Fig. 2. Some outstanding forms are classified as "spindles" (e.g., a1 = −1.8, a2 = −0.9) or as "beating tremor" (e.g., a1 = 0.1, a2 = −0.9). For $N=1$ and $t_e > t_c$, the nonoverlapping response functions will appear as a sequence of transients or wave groups. All these tremor forms are observed in recordings, although their connection with special states of volcanic activity remains an essentially unsolved problem. For $N>1$ and both cases $t_e > t_c$ or $t_e < t_c$, a time series such as Fig. 1 will be

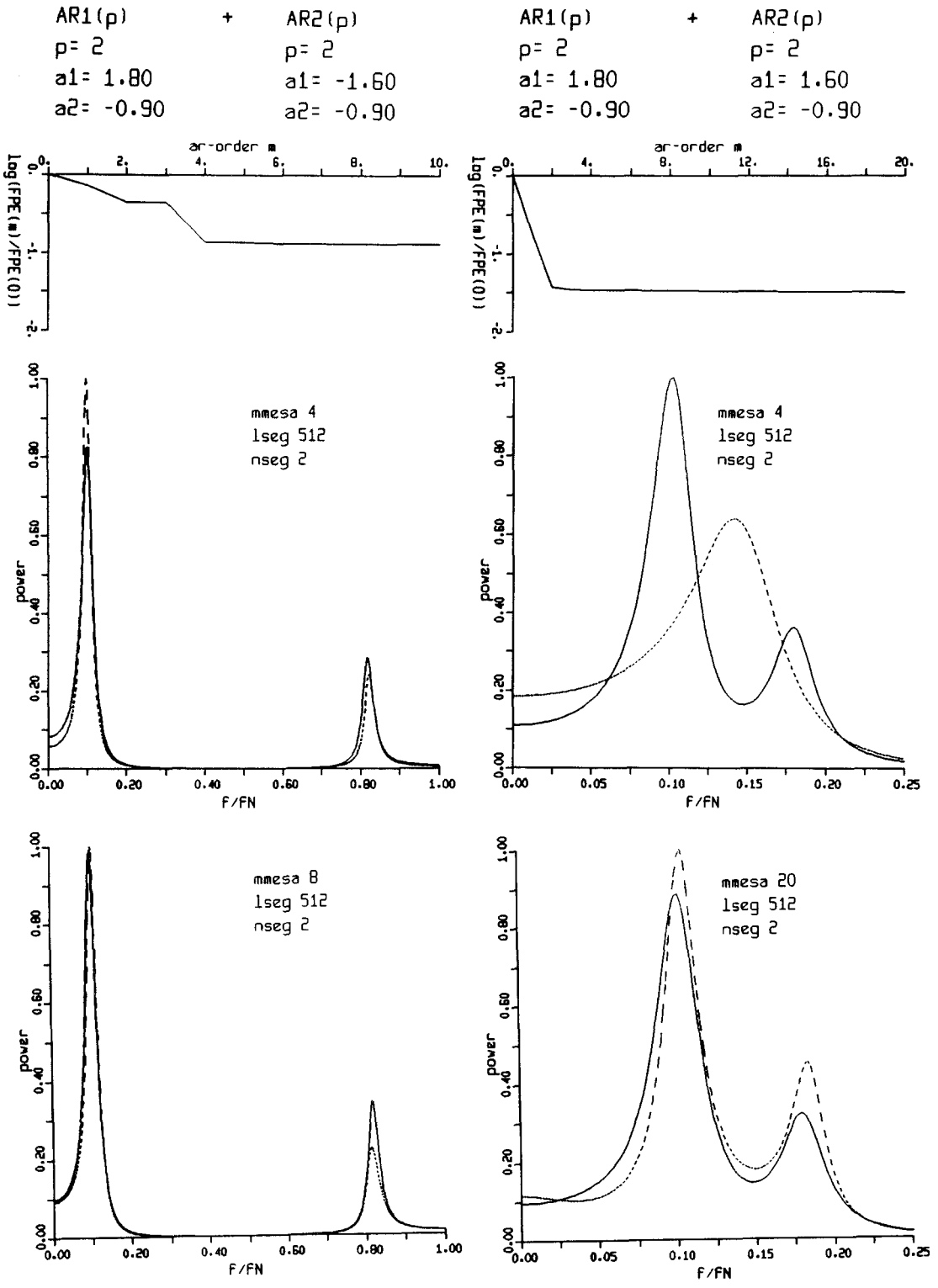

Fig. 4. Maximum entropy spectral analysis of two synthetic time series with a two-peak and a double-peak spectrum, respectively, generated by superimposing two $AR(2)$ processes. The spectrum with the higher peak amplitude is normalized to full scale in each case. Symbols as in Fig. 3. *Top.* Determination of the order of the composed AR process using the final prediction error (*FPE*) criterion. *Left.* Mesagram estimate (dashed) of the theoretical two-peak spectrum (solid) using the *FPE* order (middle). The spectrum remains stable with slowly improved approximation for increased order mmesa (bottom). *Right.* To resolve the double-peak spectrum orders mmesa higher than the *FPE* value must be used

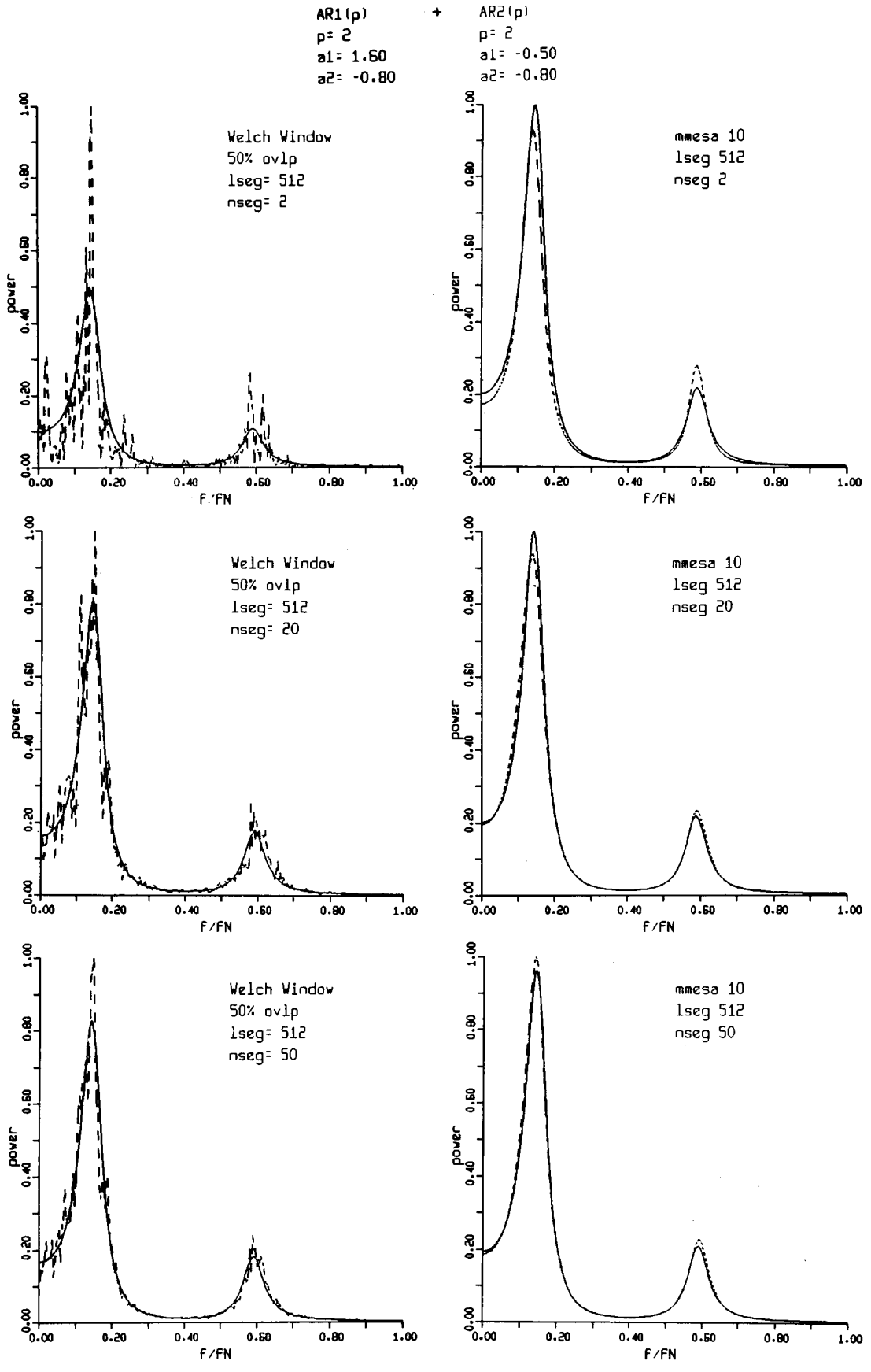

Fig. 5. Comparison of periodogram estimates and mesagram estimates of a two-peak power spectrum generated by superimposing two *AR*(2) processes. Normalization as in Fig. 4. *Left.* Periodogram estimates (method as in Fig. 1; dashed) of the theoretical spectrum *(solid);* reduction of variance with increased number of overlapped segments. *Right.* Corresponding mesagram estimates *(dashed).* No overlapping. lseg, segment length in samples; nseg, number of data segments; mmesa, order of MESA spectrum

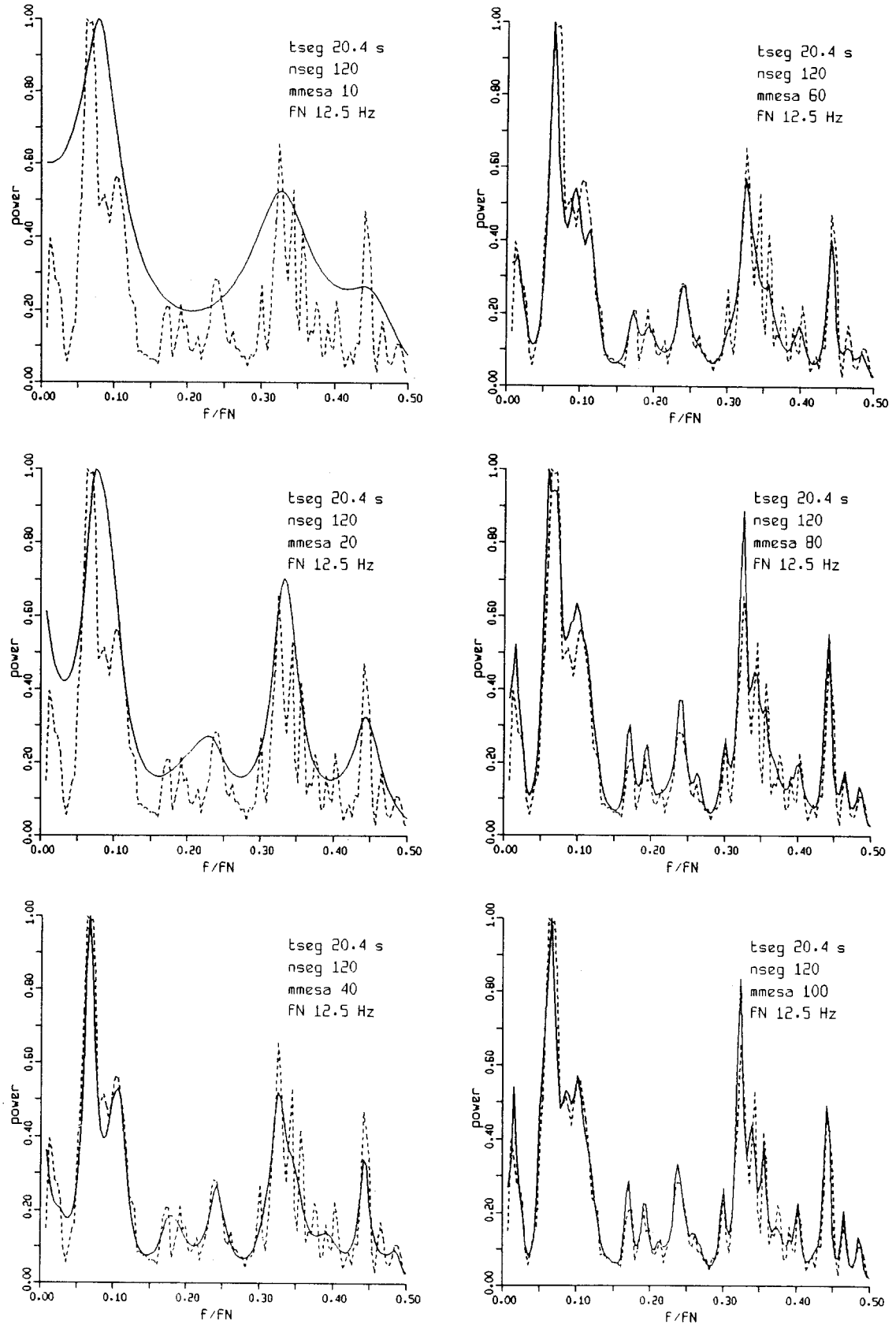

Fig. 6. Long-term mesagrams *(solid)* for increasing MESA order for the Etna tremor data, demonstrating the smoothing and resolution properties of the mesagrams and their relationship to the periodogram power spectrum *(dashed)* in Fig. 1. tseg, segment length; nseg, number of segments for mesagram estimate; mmesa, order of MESA spectrum; f_N, Nyquist frequency

observed. Transients are superimposed on a sequence of short-term stationary segments. For $N \gg 1$, the transitions between these segments will be smeared and the tremor will appear as a long-term stationary time series.

Maximum entropy spectral analysis of quasi-stationary tremor using data from Etna (Sicily)

The quasi-stationary tremor record in Fig. 1 consists of a sequence of short-term stationary segments of 5–20 sec length, characterized by small variations in the instantaneous frequencies and amplitudes. The complete data file used in the following analysis has a length of 40.8 min. The file was sectioned into 120 segments each of 20.4-s length. The MESA spectrum of a single segment is called a segment spectrum. Averaging a small number (less than about 5) of segment MESA specta results in a short-term mesagram. Averaging a large number of segment MESA spectra or segment periodograms results in a long-term mesagram or in the conventional power spectrum, respectively.

The long-term mesagrams $M(f, m)$ for the complete data file estimated for increasing orders m show a close relationship to the conventional power spectrum $P(f)$ (Fig. 6): $M(f, m)$ approaches the shape of the power spectrum$P(f)$ with increasing high order m and represents smoothed estimates of $P(f)$ at various degrees of resolution for increasing low orders. This correspondence can be used for checking the significance of split peaks observed for increasing orders. Furthermore, a low-order mesagram estimated from short tremor records provides a reasonable activity measure during times of highly fluctuating activity.

The segment MESA spectra in the time-frequency domain (Fig. 7) illustrate the two characteristics of the resonator model, i.e., narrow spectral peaks and a random excitation pattern along the time axis. Figure 7 also shows the histogram for the peak frequencies of the MESA segment spectra together with the long-term spectra from Fig. 6 for the order mmesa = 100. By relating each peak in a segment MESA spectrum to a single excitation, the histogram describes the excitation probabilities of the resonators. For an ensemble of resonators, the radiated power $P_0(f)$ in Eq. (1) can be expressed as $P_0(f)\,df = e(f)\,p_0(f)\,df$, where $e(f)$ and $P_0(f)$ are the mean values of the excitation probability and the radiation power of the resonators in the band $\{f, f+df\}$, respectively. Both parameters can be estimated from the observed power spectrum $P(f)$ and the histogram of the MESA peak frequencies if the medium transfer function $H(f)$ is known.

It is possible that two or more spectral peaks in the segment MESA spectra or in the short-term mesagrams are linked due to the excitation of higher harmonics or the coupling of the resonators or driving forces. Figure 8 shows a collection of two-segment mesagrams arranged by increasing complexity. Most of the peaks in the long-term power spectrum can be recognized in all mesagrams even at low amplitudes. Any single peak or combination of peaks can be observed in at least one segment with a high amplitude. A correlation seems to exist between the peaks in the band around 1 Hz and the high-frequency peaks above 4.0 Hz. This can be seen also in the tremor record in Fig. 1 where high-frequency wave groups (frequencies 4–5 Hz) are superimposed on the low-frequency transients (frequencies around 1 Hz). Thus, it seems possible to detect correlated excitations using short-term MESA spectra. To corroborate this observation, the correlation analysis of a larger tremor record is necessary.

If the tremor source is modelled as an ensemble of randomly excited second-order resonators, the tremor time series can be represented as a superposition of N $AR(2)$ processes, where N is the number of peaks in the mesagram for a large order m. The inversion problem for the MESA spectra then involves the determination of the $2N$ $AR(2)$ coefficients $[a1_j, a2_j, j = 1, N]$, which are related to the m AR parameters of the MESA estimation process by a set of nonlinear equations. From the AR parameters the eigenfrequencies and damping coefficients of the associated resonators can be calculated. One method of inversion is the isolation of a peak by bandpass filtering, segmenting the filter output and averaging the AR parameters for a second-order MESA spectrum. Figure 9 illustrates this method for two peaks of the power spectrum in Fig. 1.

Maximum entropy spectral analysis of beating-tremor and tremor storm using data from Merapi (central Java)

Figure 10 shows the application of MESA to a beating tremor record observed at the volcano Merapi. The segment MESA spectra in the time-frequency domain indicate that the beating tremor is radiated by the random impulsive excitation of a small number of resonators with closely adjacent eigenfrequencies around 1.75 Hz. In this case the segment spectra have not been averaged so that rapid variations of the instantaneously excited resonators can still be observed.

During phases of lava dome building and growth, nonstationary tremor storms can be observed. They are characterized by increased amplitudes and a "short rise time-long decay time" envelope. Figure 11 presents the MESA processing for a Merapi tremor storm recorded at the stations Labuhan and Kalikuning. The short-term mesagrams in the time-frequency domain show complex fine structure with excellent spatial coherence over the entire duration of the tremor storm. Two-dimensional, time-frequency, cross-correlation analysis yields a correlation coefficient of $R = 0.87$. The main maximum and the highest side maximum are located at the same frequencies for both stations. They are at 2.2 Hz and 3.5 Hz, respectively.

Figure 12 shows the corresponding MESA processing for a tremor storm about six times longer in duration. The spatial coherence is fairly good for low frequencies and for the large amplitudes at the beginning of the storm. The correlation coefficient is $R = 0.66$. If

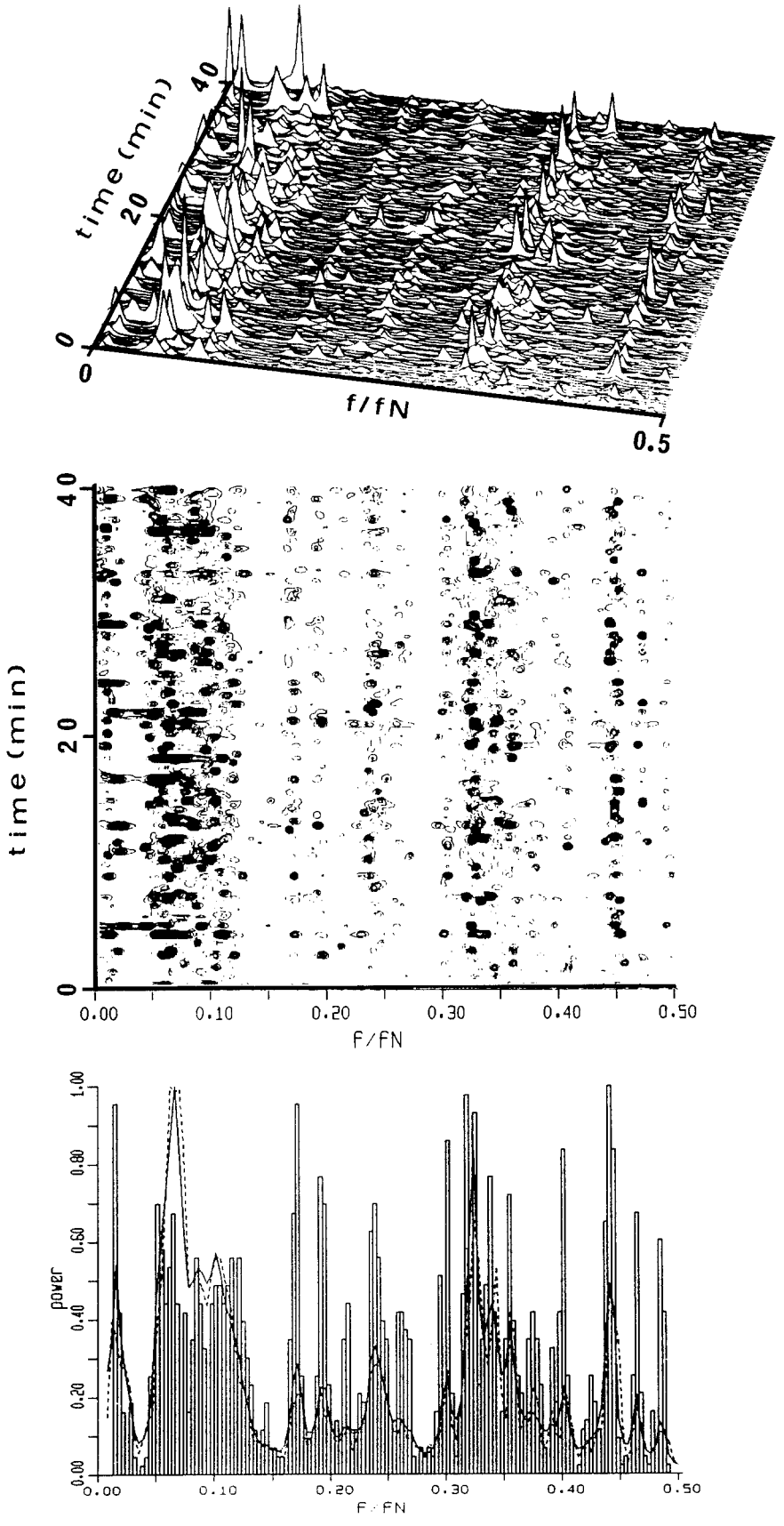

Fig. 7. Various representations of tremor MESA spectra illustrating the random and multiresonator character of the tremor sources. *Top.* Perspective view of the segment MESA spectra in the time-frequency domain for successive nonoverlapping segments of the Etna tremor data. Segment length of 20.4 sec; 120 segments; MESA order 100. *Middle.* Topographic map of the segment MESA spectra in the time-frequency domain illustrating the random character of the excitation process. *Bottom.* Histogram of the 50 strongest peaks of each segment MESA spectrum superimposed on the long-term mesagram (mmesa = 100) and the power spectrum in Fig. 6

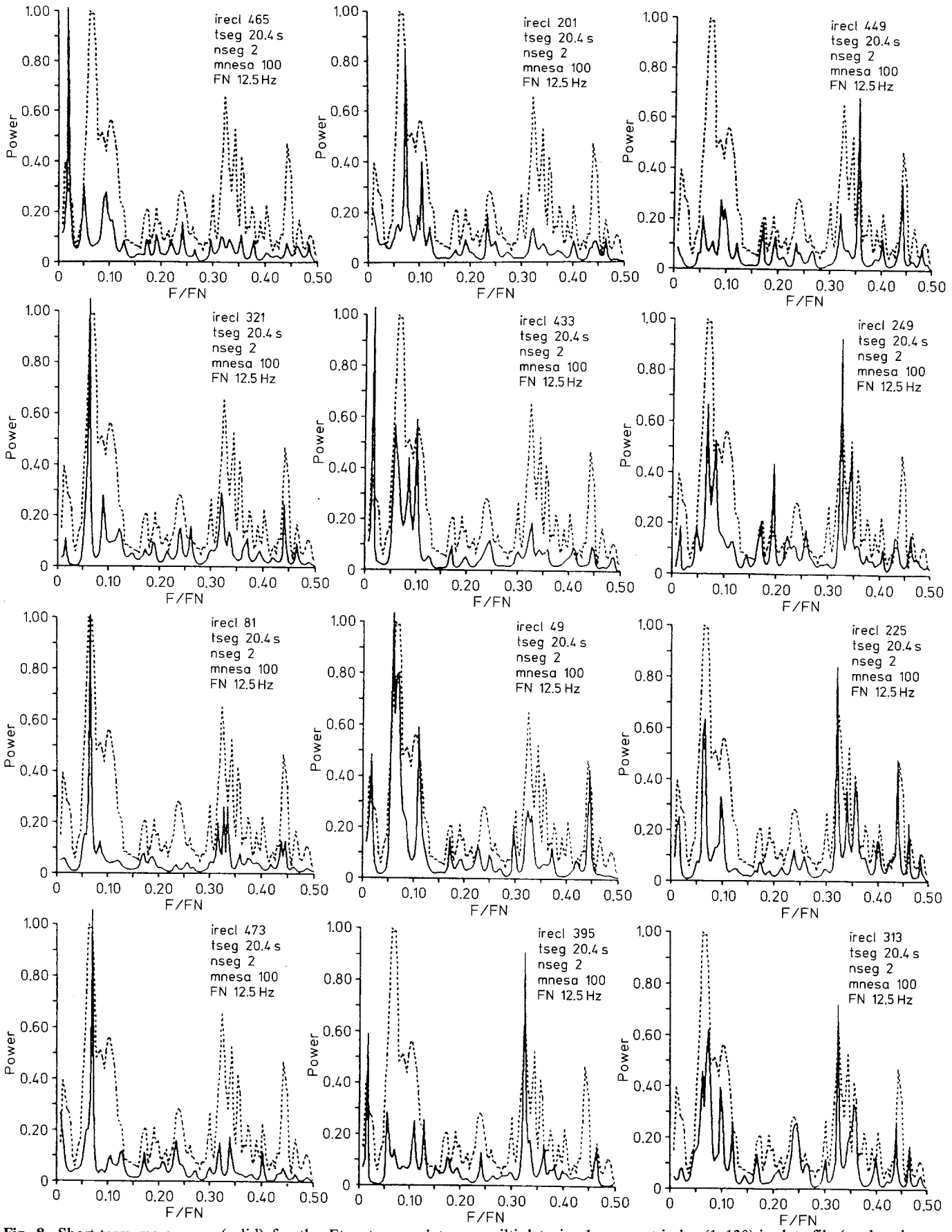

Fig. 8. Short-term mesagrams (solid) for the Etna tremor data with increasing complexity from left to right column, superimposed on the power spectrum in Fig. 1; low-frequency singlets → low-frequency miltiplets → low- and high-frequency singlets and miltiplets. irecl, segment index (1–120) in data file (analyzed section from segment irecl to segment irecl + nseg-1); tseg, segment length; nesg, number of segments for mesagram estimate; mmesa, order of MESA spectrum; f_N, Nyquist frequency

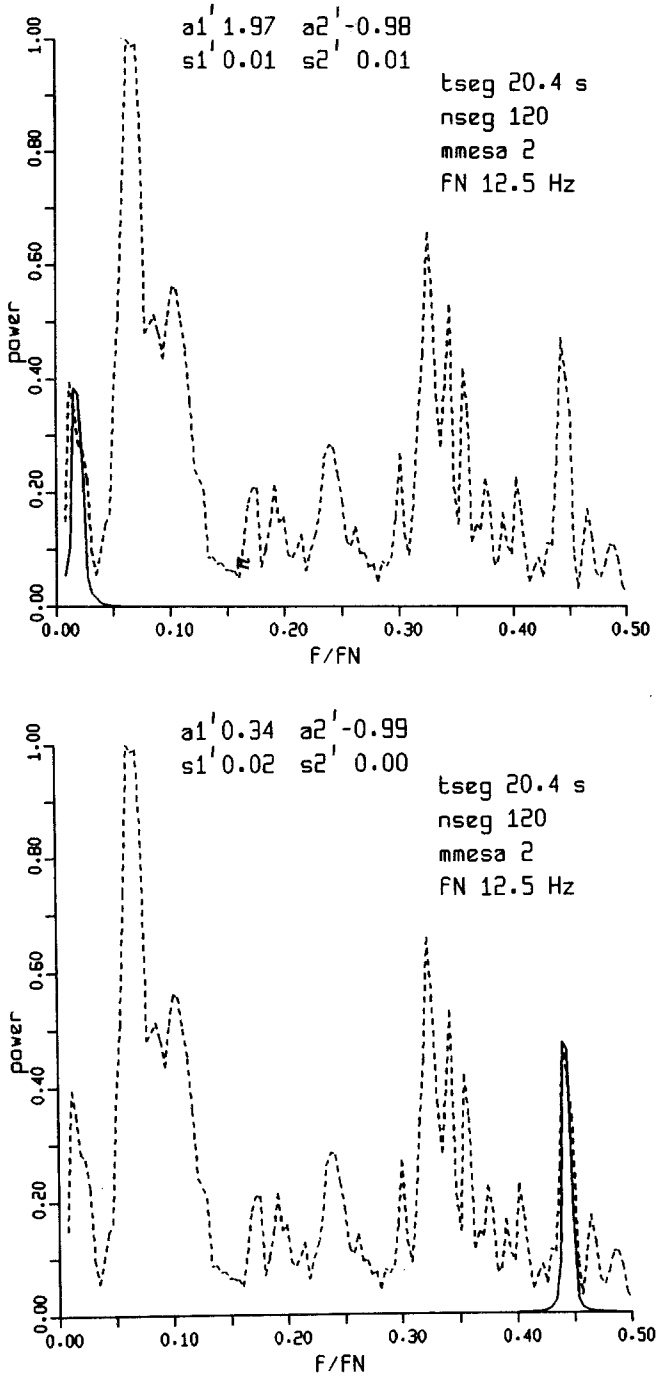

Fig. 9. Estimation of the $AR(2)$ parameters for two peaks of the power spectrum in Fig. 1 (dashed) by band-pass filtering the tremor data and averaging the AR parameters for the second-order segment MESA spectra. The long-term mesagrams (solid) of the two peaks are normalized to the peaks of the power spectrum. tseg, segment length; nseg, number of segments for mesagram estimate; mmesa, order of MESA spectrum; f_N, Nyquist frequency; a1′, a2′, estimated $AR(2)$ parameters; s1′, s2′, standard deviations of $AR(2)$ parameters

the spectrum of the station KKN is shifted slightly toward higher frequencies, a value of $R=0.73$ is obtained. Two coherent peaks at 2.2 Hz and 4.1 Hz are observed in the time interval containing large amplitude signals at the beginning of the storm. During the last interval of the storm, high frequency peaks (e.g., at 5.8 Hz and 6.3 Hz) are observed at the station Labuhan which is nearer to the crater. These peaks are greatly reduced at station Kalikuning, probably due to absorption. Further tremor storm recordings must be analyzed to determine whether time-frequency mesagrams can be used for pattern recognition and source parameter determination.

Conclusions

Considering the tremor source as an ensemble of randomly excited weakly damped resonators is a useful hypothesis for the estimation and interpretation of long-term and short-term power spectra. In addition, the association of the resonators with magma-filled conduits and dikes and of the random excitation process with degassing turbulences in the magma-gas pressure field is a widely accepted model (McNutt 1989). However, the physics of the elementary processes in the source remains an essentially unsolved problem involving the treatment of the nonlinear fluid dynamics of the two-phase magma-gas system under the complicated physical and geometrical boundary conditions inside a volcano.

Recently developed digital broad-band seismometers have increased the bandwidth and the dynamic range of tremor recordings by several orders of magnitude. The digital data can be analyzed using the powerful methods of digital signal processing. Standard methods of time series spectral analysis such as trend analysis (Martinelli 1987) and periodogram analysis (Riuscetti et al. 1977) describe the average behavior of the tremor sources for time intervals of years to hours. These methods can therefore be used for the long-term monitoring of the volcanic activity.

Although performed on a limited sample of data, this study has proven that the analysis of tremor recordings using the maximum entropy method can provide important volcanological insights.

a) Maximum entropy spectral analysis can be used to resolve peaked power spectra and to estimate autoregressive parameters from short time windows in the range from 10 seconds to a minute. This follows from the close relationship between the long-term conventional periodogram power spectrum and the various representations of MESA spectra such as the long-term mesagrams and the histograms of MESA spectra peak frequencies.

b) The mesagram calculated by segmenting the record and averaging the MESA segment spectra approaches the long-term conventional (periodogram) power spectrum with increasing order and provides smoothed estimates of this spectrum at various degrees of resolution for low orders. If it can be shown empirically that such a smoothed estimator of the multipeak power spectrum is a measure for the activity of a volcano, the AR parameters of the low-order mesagram can be easily calculated on-line and monitored. The mesagram can be considered a compressed data set to be transmitted and stored in place of the complete time series.

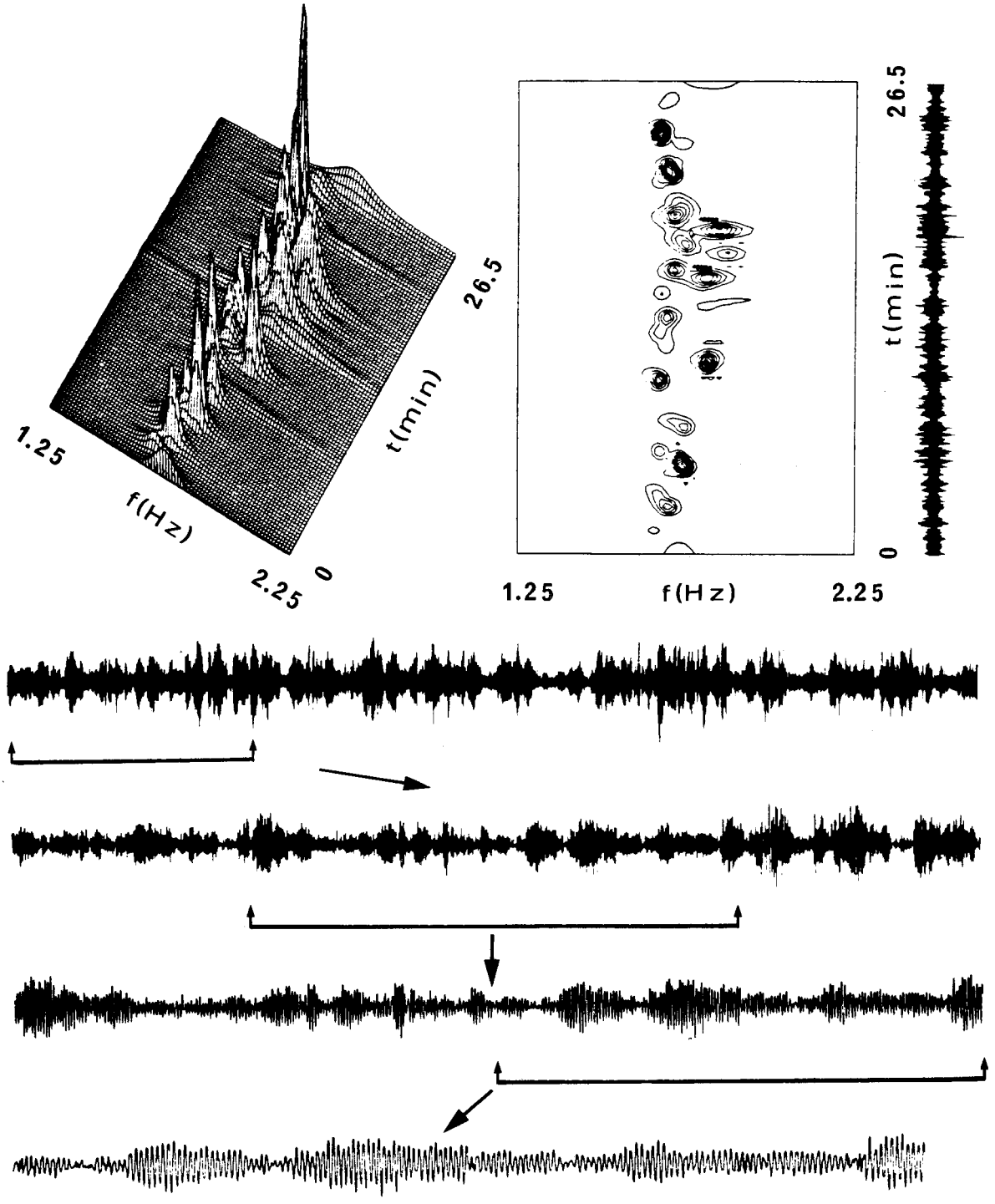

Fig. 10. Maximum entropy spectral analysis of a beating tremor recording. Segment duration, 10 sec; number of segments, 159; order of MESA spectra 10. *Bottom.* Plots of beating tremor with gradually increased time resolution for the indicated segments. Klathakan, Merapi (central Java) 1.5 km from crater on 23 May 1987. State of activity, increasing; 1 Hz seismometer with velocity transducer. *Top.* Perspective view and topographical map of the segment MESA spectra in the time-frequency domain for successive nonoverlapping data segments

c) The application of MESA analysis to a limited data set has provided a qualitative confirmation of the resonator-ensemble model. The tremor is a superposition of wavelets radiated by many randomly excited resonators. While the long-term power spectrum describes the radiation pattern of the ensemble of resonators, the short-term MESA spectra reveal the properties of the elementary resonators. By combining long-term periodogram spectra and short-term MESA spectra, new source parameters such as eigenfrequencies and damp-

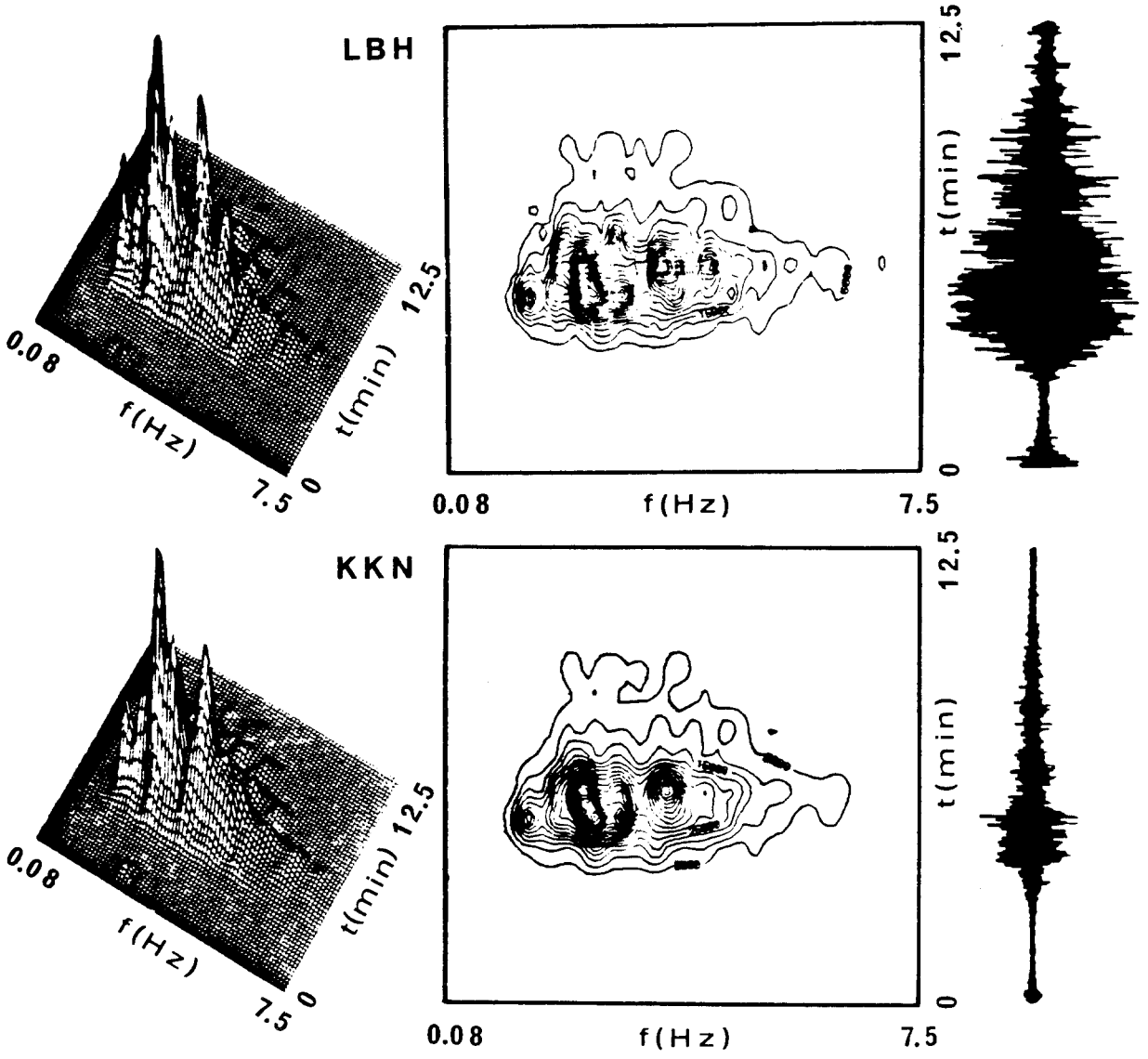

Fig. 11. Perspective view and topographical map of the short-term mesagrams in the time-frequency domain for a Merapi tremor storm recorded at the stations Labuhan (LBH; 2.5 km from crater) and Kalikuning (KKN; 5.0 km from crater). 13 October 1986. State of activity, lava dome growing; 1 Hz seismometer with velocity transducer. Segment length, 12.5 sec; number of nonoverlapping segments for mesagram estimate, 4; oder of MESA spectra, 100

ing coefficients of single resonators, excitation probabilities, resonator coupling, and the correlation of driving forces can determined.

Because the time series investigated were short, the application of the MESA method to the short-term monitoring of volcanic activity and the determination of tremor source parameters has only been demonstrated qualitatively. Furthermore, three unsolved problems, i.e., the determination of the tremor wavefield kinematics, the medium transfer function, and the source location, currently prevent the complete interpretation of tremor power spectra. Using bandpass filtered tremor data of a three-component station, polarization analysis might reveal dominant azimuths and angles of incidence for the various resonator bands. This method can also resolve the composition of the tremor wavefield in terms of body and surface waves. The tremor source locations could then be determined from a network of three-component stations using polarization data and amplitude-distance functions.

Acknowledgements. We gratefully acknowledge the support provided by the Kernforschungsanlage Jülich and by the Badan Pengkajian Dan Penerapan Teknologi. The computer hardware at the Geophysics Laboratory of the Gadjah Mada University in Yogyakarta was donated by the Dewan Konsortium Penndidikan Pertamina Kontraktor Produktion Sharing. The first author thanks the Federal Institute for Geosciences and Natural Resources (Federal Republic of Germany) for supporting two research stays at the Gadjah Mada University. The volcanic tremor data of Etna were recorded by R Schick using the Wielandt-Streckeisen seismograph available at the Istituto di Science della Terra, Catania. We thank Prof. Mugiono for many stimulating discussions and M Hellweg for critically reading the manuscript and offering many valuable suggestions.

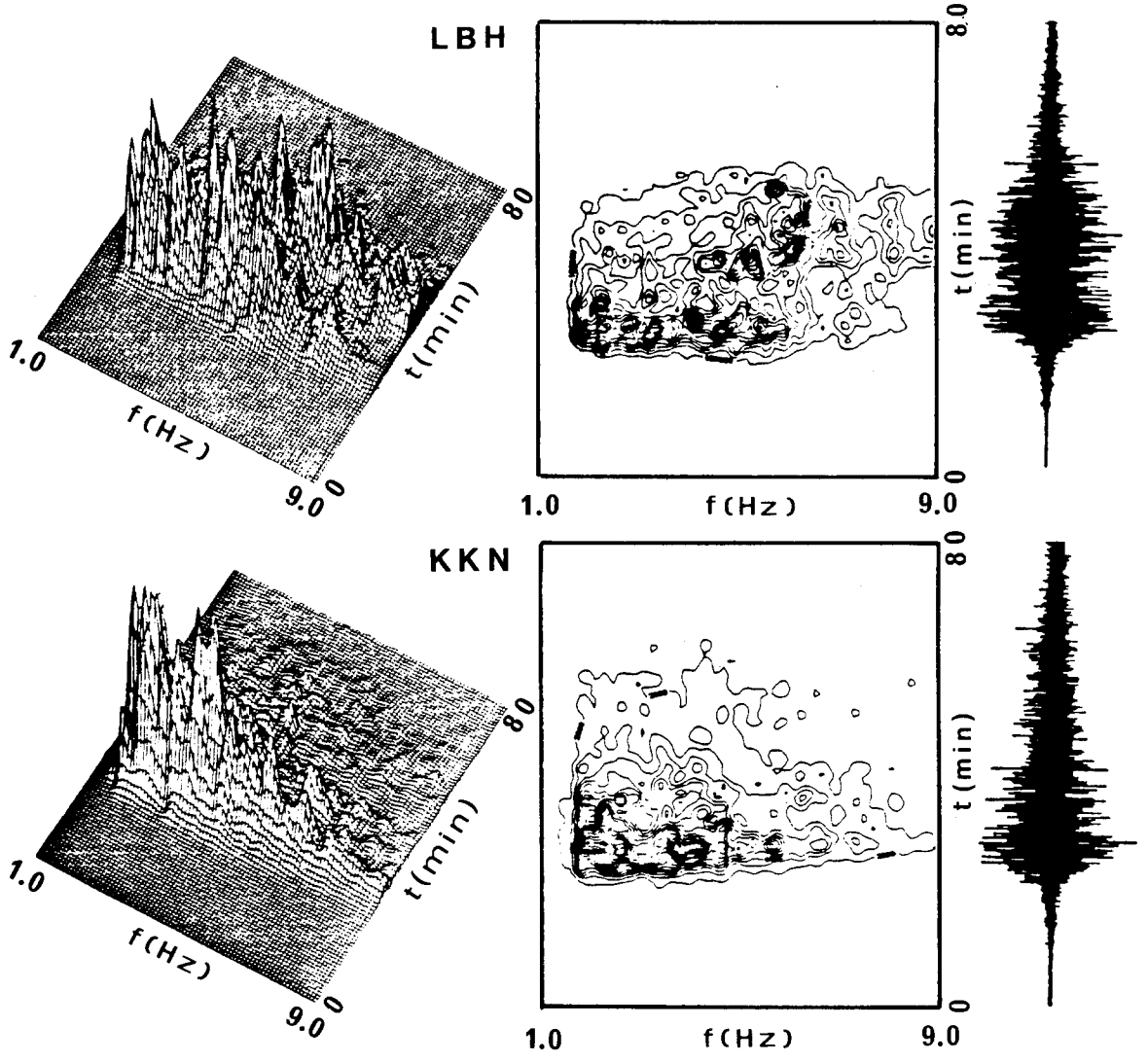

Fig. 12. Perspective view and topographical map of the short-term mesagrams in the time-frequency domain for a Merapi tremor storm recorded at Labuhan (LBH; 2.5 km from crater) and Kalikuning (KKN; 5.0 km from crater). The records and spectra are normalized to their maxima. 27 February 1985. State of activity, lava dome growing; 1 Hz seismometer with velocity transducer; Segment length of 20 sec; number of nonoverlapping segments for mesagram estimate, 4; order of MESA spectra 100

References

Akaike H (1974) A new look at the statistical model identification. IEEE Trans AC-19:716–723

Andersen N (1974) On the calculation of filter coefficients for maximum entropy spectral analysis. Geophysics 39, 1:69–72

Box GEP, Jenkins MG (1976) Time series analysis, forecasting and control. Holden-Day, San Francisco pp 1–575

Burg JP (1967) Maximum entropy spectral analysis. Presented at the 37th Annual International SEG meeting, Oklahoma City Reprint in: Childers (1978): Modern spectral analysis, IEEE Press, 34–41, New York, pp 34–41

Chen WY, Stegen GR (1974) Experiments with maximum entropy power spectra of sinusoids. J Geophys Res 79, 20:3019–3022

Childers DG (ed) (1978) Modern spectrum analysis. IEEE Press, New York, pp 1–334

Clearbout JF (1976) Fundamentals of geophysical data processing. McGraw-Hill, New York pp 1–274

Gutowski PR, Enders AR, Treitel S (1975) Spectral estimation: Fact or fiction. IEEE Trans GE-16:80–84

Haykin S (ed) (1979) Nonlinear methods of spectral analysis. Springer, Berlin Heidelberg New York pp 1–247

Jenkins GM, Watts DG (1969) Spectral analysis and its applications. Holden-Day, San Francisco pp 1–525

Kanasewich ER (1981) Time sequence analysis in Geophysics. The University of Alberta Press, Edmonton, pp 1–480

Priestly MB (1981) Spectral analysis and time series. Academic Press, London, pp 1–890

Press WH, Flannery BP, Teukolsky SA, Vetterling WT (1986) Numerical Recipes. Cambridge University Press, Cambridge pp 1–818

Martinelli B (1987) Seismic patterns observed at 'Nevado del Ruiz' in the period August–September 1985. In: Int Workshop 'Forced Fluid Flow'. Commission European Comm, EUR 11164/1

McNutt SR (1989) Volcanic tremor from around the world. Abstract, EOS Transactions, American Geophysical Union 70, No 43, p 1189

Riuscetti M, Schick R, Seidl D (1977) Spectral parameters of volcanic tremors at Etna. J Volcanol Geotherm Res 2:289–298

Schick R (1988) Volcanic tremor-source mechanism and correlation with eruptive activity. Natural Hazard 1:125–144

Ulrych TJ, Bishop TN (1975) Maximum entropy spectral analysis and autoregressive decomposition. Rev Geophys 13:183–200